Structural Changes of Silica Mesocellular Foam Supported Amine-Functionalized CO_2 Adsorbents Upon Exposure to Steam

Wen Li, Praveen Bollini, Stephanie A. Didas, Sunho Choi, Jeffrey H. Drese, and Christopher W. Jones*

School of Chemical & Biomolecular Engineering, Georgia Institute of Technology, 311 Ferst Drive, Atlanta, Georgia 30332, United States

ABSTRACT Three classes of amine-functionalized mesocellular foam (MCF) materials are prepared and evaluated as CO_2 adsorbents. The stability of the adsorbents under steam/air and steam/nitrogen conditions is investigated using a Parr autoclave reactor to simulate, in an accelerated manner, the exposure that such adsorbents will see under steam stripping regeneration conditions at various temperatures. The CO_2 capacity and organic content of all adsorbents decrease after steam treatment under both steam/air and steam/nitrogen conditions, primarily due to structural collapse of the MCF framework, but with additional contributions likely associated with amine degradation during treatment under harsh conditions. Treatment with steam/air is found to have stronger effect on the CO_2 capacity of the adsorbents compared to steam/nitrogen.

KEYWORDS: CO_2 capture • supported amine • deactivation • steam stability;

INTRODUCTION

The increasing CO_2 concentration in the atmosphere is considered a leading contributor to global climate change in the past century (1, 2). As a result, increased attention has been paid to the development of methods to reduce anthropogenic CO_2 emissions to the atmosphere. The benchmark process for carbon capture from large point sources is based on use of liquid amine/water solutions to absorb CO_2 from a postcombustion exhaust stream, with the solvents being regenerated by an energy-intensive steam-stripping technique. This approach is often characterized as having high cost and low energy efficiency, although it should be noted that significant advances in cost-reduction and optimization have been achieved in recent years (3−7). In parallel, the development of processes based on solid adsorbents have been considered as alternative separation technologies for postcombustion CO_2 capture. Compared to the liquid amine/water process, the alternative solid adsorbent could provide several advantages, such as elimination of corrosion problems associated with the liquid amine, as well as decreasing the energy cost for sorbent regeneration (7).

Among various solid CO_2 adsorbents being evaluated, amine-functionalized adsorbents using mesoporous oxide materials as substrates show promising properties such as low operating temperatures (ambient-75 °C) and large adsorption capacities in the presence of water due to strong interactions between CO_2 and the amine sites. In general, there are three classes of supported amine sorbents that have been widely investigated. Class 1 adsorbents were first investigated by Song in 2002 (8−13), and are most often composed of polymeric amines [e.g., poly(ethyleneimine), PEI] that are physically impregnated into/onto porous supports (14−19). Class 2 adsorbents, based on amines that are covalently linked to the solid support, are perhaps the most well-studied class of supported amine adsorbent materials. They were first reported for CO_2 adsorption by Tsuda in 1992 (20, 21), and can be prepared by grafting of silanes to preformed silica or cocondesation of the amine-containing silanes with traditional silica precursors, such as tetraethyl orthosilicate (TEOS). Prior to these applications, silica materials containing grafted amine groups were well-known in other applications, such as catalysis (22), adsorption of biomolecules (23) or adsorption of metal cations (24). Adsorbents of this type are most often prepared by binding amines to oxides via the use of silane chemistry (25−41) or via preparation of polymeric supports with amine-containing side chains (42−44). Sayari's (45−52) group has done extensive work related to this class of adsorbents. Our group reported the first class 3 adsorbents for CO_2 capture in 2008 (53, 54) class 3 adsorbents are made by in situ polymerization of an amine-containing monomer on porous supports, leading to covalently grafted polymers on the support. The hyperbranching surface polymerization of aziridine on flat substrates was first reported by Kim and co-workers (55), and then adapted to porous silicates by Rosenholm et. al (56, 57) and our group (53).

Because most of the research on amine-functionalized adsorbents has focused on maximizing the CO_2 adsorption capacity, simple sorbent regeneration methods that are not practical in real processes, such as temperature swing in an inert gas purge, have been used (7, 58). Our group recently

* Corresponding author. E-mail: christopher.jones@chbe.gatech.edu.
Received for review August 25, 2010 and accepted October 21, 2010

DOI: 10.1021/am100786z

reported the first description of steam-stripping for the regeneration of CO_2-loaded supported amine adsorbents (58). In that preliminary contribution, all three classes of adsorbents could be fully regenerated through a steam stripping procedure that utilized very low temperature steam (105 °C) over several cycles.

However, it can be anticipated that steaming silica-supported amine materials may lead to significant structural changes in the solids. Indeed, it is well-established that the hydrothermal/steam stability of amorphous silica materials can be problematic, and that the stability is a function of the materials heteroatom content (e.g., Al, B, etc.) (59, 60), wall thickness (61), thermal treatments (62), and surface functionalities (63−65), among other factors. Furthermore, there is no literature available reporting the stability of any of the three classes of CO_2 adsorbents under steaming conditions. In this study, sorbents of all three classes of aminosilica materials based on silica mesocellular foam (MCF) supports were prepared and treated under accelerated steaming conditions under steam/air and steam/nitrogen at various temperatures using an autoclave reactor. The physical and chemical properties of the adsorbents before and after steam treatment were investigated by scanning electron microscopy (SEM), nitrogen physisorption, thermal gravimetric analysis (TGA), and FT-IR and FT-Raman spectroscopies. The CO_2 adsorption capacities of the solids were measured before and after exposure to the various steaming conditions to evaluate the treatments on the capacity of the adsorbents.

EXPERIMENTAL MATERIALS AND METHODS

Materials. Pluronic P123 EO-PO-EO triblock copolymer, trimethylbenzene (TMB, 97%), tetraethyl orthosilicate (TEOS, 98%), low molecule-weight poly(ethyleneimine) (PEI, $M_n \approx 600$, $M_w \approx 800$), methanol (99.8%), ethanol (99%), anhydrous toluene (99.5%), 3-aminopropyltrimethoxysilane (APTMS, 97%), and 3-(trimethoxysilyl)propylethane diamine (AEAPTMS, 97%) were purchased from Aldrich. Concentrated HCl was purchased from J. T. Baker.

Synthesis of Amine-Functionalized MCF. For the preparation of all the adsorbents, lab-synthesized mesocellular foam (MCF) silica was used as the support. In a typical synthesis, 16 g of Pluronic P123 was used as a structure-directing agent and was dissolved in 260 g DI-water with 47.1 g concentrated HCl. Then 16 g of TMB was added at 40 °C and stirred for 2 h before 34.6 g of TEOS was added to the solution. The solution was kept at 40 °C for 20 h before 184 mg NH_4F (in 20 mL DI-water) was added. The mixture was later aged at 100 °C for another 24 h. The resulting silica was filtered, washed with DI-water, dried in oven, and calcined at 550 °C in air for 6 h to remove the organic template before further use (66, 67). Before the adsorbent syntheses, the calcined MCF was first dried under vacuum at 100 °C for 24 h to remove absorbed water.

For the preparation of the Class 1 adsorbent, 1.2 g of low-molecular-weight PEI and 60 mL methanol were mixed first in a 150 mL flask for 1 h. Subsequently, 2 g of MCF silica was added and stirred for an additional 12 h. The methanol solvent was later removed by rotavap, and the resulting adsorbent (MCF-PEI) was further dried under a vacuum at 75 °C overnight before testing.

For preparation of the Class 2 adsorbent (MCF-Mono and MCF-DMA), MCF was functionalized through the reaction of organosilanes with surface silanols. First, 60 mL of anhydrous toluene and 2 g of MCF was mixed in a 150 mL pressure vessel for 1 h, and then 2 g of either APTMS or AEAPTMS was added into the mixture. The mixture was kept under vigorous stirring for 24 h at room temperature. The resulting adsorbent (MCF-DMA and MCF-Mono) was recovered by filtration, washed with toluene and acetone, and then dried under vacuum at 75 °C overnight.

For the Class 3 adsorbent, MCF was reacted with aziridine in a similar manner as reported in the literature (53). **Note**: *Aziridine is highly reactive and toxic!* For this synthesis, 3 g of MCF was dispersed in 90 mL of toluene in a 150 mL pressure vessel and the mixture was stirred for 1 h before 6 g of aziridine (which was synthesized in the lab (53, 68) and immediately used), was added. After continuous stirring for 24 h, the resulting adsorbent (MCF-HAS) was filtered, washed with toluene and ethanol, and dried under a vacuum at 75 °C overnight. The synthesis methods are depicted in Scheme 1.

Steam/Air and Steam/Nitrogen Treatment of Adsorbents. An autoclave from Parr Instruments was used to treat the adsorbents under steam/air or steam/nitrogen conditions, as depicted in Scheme 2. For both conditions, typically, a glass tube was filled with 0.3 g of amine-functionalized adsorbent and then put into a glass beaker that was filled with approximately 30 mL of DI water. The beaker was then placed in the autoclave. After sealing the autoclave, air or nitrogen gas was purged through the autoclave for 2 h. The autoclave was then sealed and heated to the desired temperature (106−180 °C) and kept at the desired temperature for 24 h. The steam pressure inside the autoclave was autogenous and monitored by a pressure transducer. When the autoclave was opened after cooling down to room temperature, no liquid water was observed to have accumulated in the sample tube, suggesting the solids were contacted with water vapor only and not liquid water. The samples were then transferred to a vacuum oven and dried at 90 °C overnight before further characterization. After steam treatment, the samples were further designated by their treatment temperature and atmosphere. For example, MCF-PEI-106-Air corresponds with the MCF-PEI sample treated at 106 °C in steam/air.

Characterization Methods. Pore characteristics of the bare silica support and the amine-functionalized adsorbents were assessed via nitrogen physisorption analysis at 77 K using a Micromeritics ASAP 2010 after drying adsorbents under vacuum at 90 °C overnight. The scanning electron microscopy (SEM) images of MCF samples were obtained using a Hitachi S800 SEM instrument. The amine loadings were determined by TGA using a Netzsch STA409. Total organic loading was estimated as the weight percentage loss from 160 to 760 °C under air atmosphere, and the results were further normalized by assuming all the organic content was combusted upon reaching 760 °C. FT-IR spectroscopy using KBr pellets and FT-Raman spectroscopy on the powders were obtained on a Bruker Vertex 80v optical bench with a RAMII Raman module.

CO_2 Capacity Measurement under Anhydrous Conditions. CO_2 adsorption measurements were performed using a computer controlled TGA Q500 from TA Instruments. The adsorption temperature was set at 45 °C and the adsorption time was set for 3 h for all adsorbents. A mixed gas consisting of 10% CO_2 in argon was used as the test gas. The weight difference before and after introducing the CO_2 mixture gas was used to calculate the CO_2 capacity. The regeneration of adsorbents was performed at 110 °C under dry nitrogen for 3 h.

RESULTS AND DISCUSSION

Steam Stability of MCF. MCF is known to be an amorphous silica with well-defined, uniform spherical pores (typically 20−45 nm) (69) that are interconnected by cylindrical windows (8−25 nm), resulting in a highly porous solid with thin walls and high BET surface areas (70, 71). Further-

Scheme 1. Synthetic Approaches to Prepare Various Amine-Functionalized Silica Mesocellular Foam (MCF) Materials: Top, Class 1 Adsorbent; Middle, Class 3 Adsorbent; Bottom, Class 2 Adsorbents

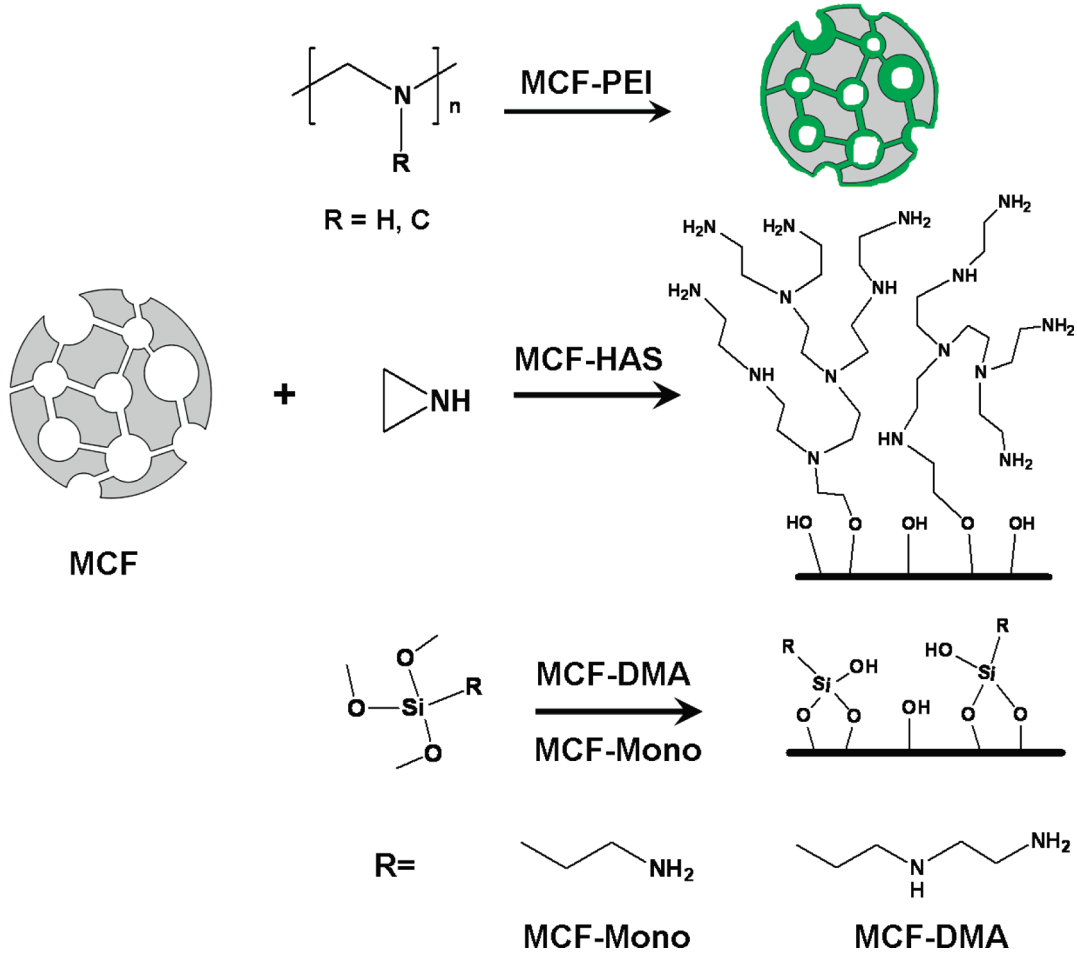

Scheme 2. Schematic Configuration of the Steam Treatment Apparatus

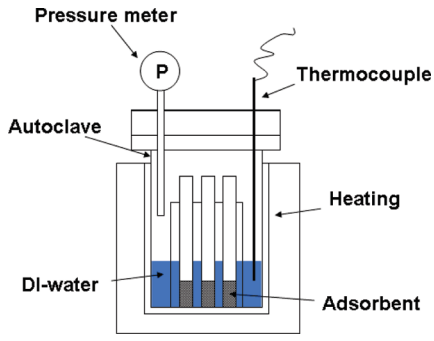

more, the 3-D mesopores in MCF are substantially larger than those of ordered mesoporous silica, such as SBA-15 (72) and MCM-41 (73). These properties of MCF may provide more favorable conditions for mass diffusion. Therefore, MCF was chosen as the substrate to prepare amine-functionalized adsorbents for this work. Although the stability of typical mesoporous silica substrates (e.g., SBA-15 and MCM-41) has been studied under hydrothermal conditions (74−79), the stability of MCF in steam is not yet well understood.

In this study, an autoclave was first used to treat bare MCF (free of organic content) at various temperatures in a steam/air atmosphere and the morphology and microstructure changes of the samples were assessed after the treatment. The nitrogen physisorption results are summarized in Table 1. As listed in the table, the calcined MCF showed a BET surface area of 615 m^2/g, an average pore volume of 2.64 cm^3/g, and average window and cell diameters of 12 and 50 nm. After the steaming treatment, the pore size and window size increased and the BET surface area and pore volume decreased, indicating the mesoporous structure of the silica substrate was not fully stable under these steaming conditions. Moreover, increased microstructural change of the MCF was observed with increasing treatment temperatures. After treating the MCF at 120 °C in steam/air, the BET surface area and pore volume of the MCF sample decreased to about 50% of the values of the original calcined sample.

Table 1. Nitrogen Physisorption Characterization of the MCF after Treatment in Steam/Air at Various Temperatures

treatment temperature	calcined	106 °C	112 °C	120 °C	180 °C
SA_{BET} (m^2/g)	615	506	342	182	47
d_{cell} (nm)	50	50	50	80	
d_{window} (nm)	12	13	15	26	
V_{pore} (cm^3/g)	2.64	2.42	2.33	1.46	0.21

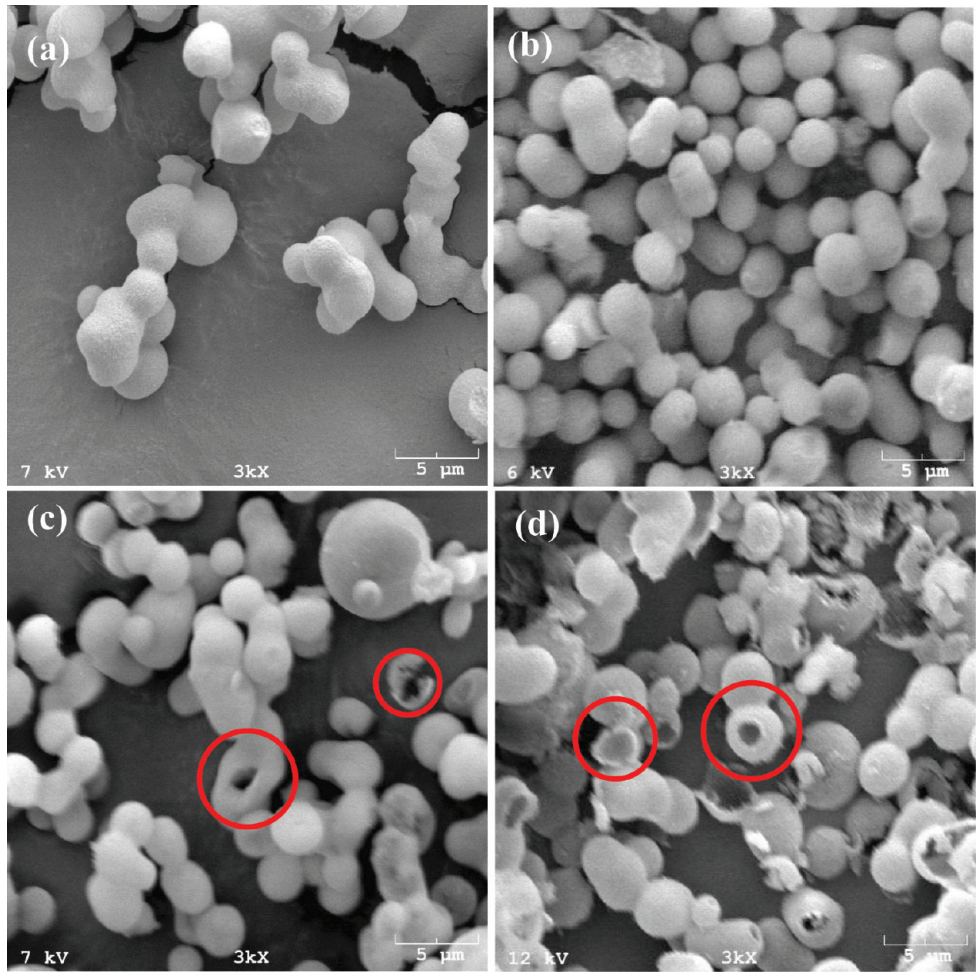

FIGURE 1. SEM images of MCF substrate particles before and after steam/air treatment at various temperatures (a) calcined; (b) steam treatment at 106 °C; (c) steam treatment at 120 °C; (d) steam treatment at 180 °C.

Furthermore, the microstructure of the MCF appeared to have almost completely collapsed after steam/air treatment at 180 °C.

The structural collapse of the MCF can be visually observed in SEM images, as shown in Figure 1. The calcined MCF particles were mostly spherical. The collapse of their spherical shape was found after treatment at 120 °C. Further collapse was observed after treatment at 180 °C. It should be noted that there is one other study of the steam stability of MCF materials reported in the literature. In that work, Zhao and co-workers heated the MCF sample to 600−800 °C in a tube furnace while flowing water was simultaneously introduced to the quartz tube by connection of a heated flask containing deionized water. The treatment continued for 3−12 h at approximately atmospheric pressure (69). This produced conditions with a low steam partial pressure and very high temperature, conditions different from what was used here.

As the goal of our work is to estimate the steam-stability of supported amine adsorbent materials upon prolonged exposure to steam and steam/oxygen, we sought to use much harsher conditions to accelerate any chemical changes that might be induced by exposure to steam/nitrogen or steam/air in a real postcombustion separation process. To this end, we used higher pressures of steam (10 bar for 180 °C steam treatment) than Zhao (<1 bar), while working in the temperature regime that is relevant to use of supported amine materials in hypothetical postcombustion CO_2 capture processes (100−200 °C).

The poor structural stability of the MCF may be inherent to its structure, as it has a high BET surface area and relatively thin walls, compared to some common ordered mesoporous silicas (SBA-15, MCM-41) or commercial silica supports.

Stability of Amine-Based MCF under Steam Treatment. On the basis of the the above results from treatment of the MCF substrate alone, the focus of the studies directed at the effect of temperature during steam treatments of the supported amine adsorbents was set to the temperature range of 106−120 °C. However, to investigate the effect of oxygen with steam on the stability of the MCF-supported amine adsorbents, all three classes of adsorbents were treated under steam/air under a wider temperature range (106−180 °C). The organic content, physical properties, CO_2 adsorption capacity, and change in the amine groups of the adsorbents before and after the steam treatment are described below.

Figure 2 compares the apparent organic content of the adsorbents, as estimated by TGA, before and after steam

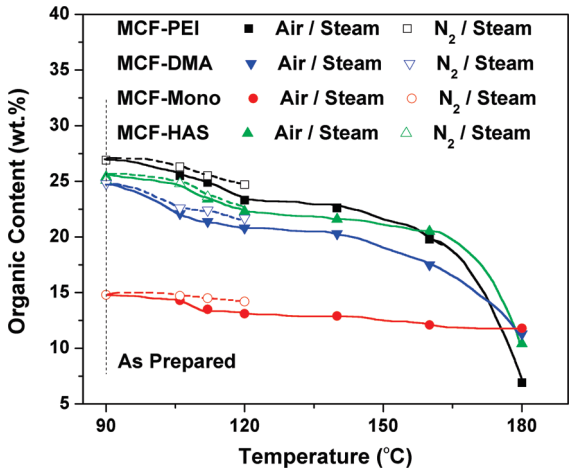

FIGURE 2. Comparison of organic content of amine-functionalized MCF before/after steam treatment under different atmospheres at various temperatures, as estimated by TGA.

treatments. As noted above, the "apparent" organic content was estimated by the weight loss in the 160−760 °C region. An apparent loss of organic content can be associated with less organic in the material after treatment, or a loss of other species, such as firmly bound water, that might be expelled from the support in the same temperature region. Such a water loss is expected to be small, if it is present at all.

In both air and nitrogen atmospheres, the organic content decreased slowly with increasing steam treatment temperature below 160 °C, and a large loss of organic content was further observed after steam/air treatment at 180 °C for all the adsorbents except MCF-Mono. This result suggests that MCF-Mono is more stable than the other three adsorbents under the present steam treatment conditions, showing exceptional stability at high temperatures upon exposure to air. Furthermore, at the same steam treatment temperature, the apparent organic content loss of the adsorbents after steam/air treatment was higher than after steam/nitrogen treatment, likely due to amine oxidation associated with the oxygen in the air.

To further understand the effect of steam treatment on the stability of the adsorbents, the CO_2 capacities of the three classes of adsorbents were measured using TGA with 10% CO_2 balanced by argon at 45 °C. The average capacities (mmol CO_2/g adsorbent) of the adsorbents over 3 cycles are summarized in Table 2. For class 1 and 2 adsorbents, the initial capacities of the as prepared samples were related to the organic content, with higher organic (amine) loadings leading to higher initial capacities. For the class 3 adsorbent, a lower CO_2 capacity than expected was achieved based on past work on HAS materials (53). This observation may be associated with several factors, including the measurement of dry capacities by TGA (dry capacities are routinely lower for supported amine materials compared to humid capacities) and use of a different substrate compared to past work (MCF vs SBA-15). After treating the adsorbents under both steam/air and steam/nitrogen conditions, the capacity of all four adsorbents decreased. Surprisingly, the capacity of all the adsorbents decreased even after treatment under the mildest conditions, in steam/nitrogen atmosphere at 106 °C. This indicates that exposure of these adsorbents to steam under very mild conditions, in an inert gas atmosphere, can lead to degradation of the adsorbents.

The amount of CO_2 adsorption capacity lost increased with increasing treatment temperature for all three classes of adsorbents, demonstrating the expected temperature effect of the steaming conditions on the capacity of the amine based adsorbents. Furthermore, the capacity loss of the adsorbents after treatment under steam/air conditions was always higher than after treatment under steam/nitrogen conditions at the same treatment temperature, demonstrating that the oxidation of the amine groups may also play a role under these conditions. For example, the capacity of the MCF-PEI adsorbent decreased from 1.26 mmol CO_2/g adsorbent to 0.91, 0.81, and 0.32 mmol CO_2/g adsorbent after treatment in steam/air at 106, 112, and 120 °C respectively, and 1.03, 0.95, and 0.82 mmol CO_2/g adsorbent after treatment in steam/nitrogen at 106, 112, 120 °C. Interestingly, although the initial CO_2 capacity of the MCF-HAS adsorbents was relatively low compared to the other types of adsorbents, it appeared to be the least affected, with the capacity remaining almost the same after steam/nitrogen treatment and only becoming slightly decreased after steam/air treatment up to 120 °C.

The data suggest there may be some stability advantage to use of adsorbents containing polymeric amines. As noted above, the MCF-HAS material showed little capacity loss after steam treatments. In addition, the MCF-PEI had a similar

Table 2. Comparison of CO_2 Capacity (mmol CO_2/g adsorbent) of Various Amine-Functionalized MCF Materials after Treatment under Steam/Air and Steam/Nitrogen at Various Temperature

				CO_2 capacity after treatment (mmol CO_2/g adsorbent)		
	organic loading (wt %)	initial CO_2 capacity[a] (mmol CO_2/g adsorbent)	treatment atmosphere	106 °C[b]	112 °C[b]	120 °C[b]
MCF-PEI	26.9	1.26	air	0.91	0.81	0.32
			nitrogen	1.03	0.95	0.82
MCF-Mono	14.8	0.78	air	0.39	0.33	0.22
			nitrogen	0.56	0.46	0.35
MCF-DMA	24.8	1.25	air	0.62	0.42	0.18
			nitrogen	0.82	0.74	0.48
MCF-HAS	25.4	0.47	air	0.41	0.40	0.39
			nitrogen	0.44	0.42	0.39

[a] Capacity without steam treatments. [b] Treatment temperature.

Table 3. Comparison of Characterization by Physisorpton of the Amine-Functionalized MCF at Various Steam Treatment Conditions: (a) MCF-PEI, (b) MCF-HAS, (c) MCF-DMA, and (d) MCF-Mono

		steam/air			steam/nitrogen		
	fresh sorbent	106 °C	112 °C	120 °C	106 °C	112 °C	120 °C
			(A) MCF-PEI				
SA_{BET} (m^2/g)	201	72	62	18	76	58	26
d_{cell} (nm)	45	52	58		53	60	
d_{window} (nm)	12	23	26		23	26	
V_{pore} (cm^3/g)	1.54	0.58	0.37	0.06	0.73	0.42	0.13
			(B) MCF-Mono				
SA_{BET} (m^2/g)	289	84	74	56	98	73	54
d_{cell} (nm)	49	52	90		49	95	
d_{window} (nm)	12	24	28		21	30	
V_{pore} (cm^3/g)	1.85	0.62	0.38	0.04	0.86	0.63	0.25
			(C) MCF-DMA				
SA_{BET} (m^2/g)	183	78	55	46	142	103	62
d_{cell} (nm)	35	39	42	60	42	45	56
d_{window} (nm)	12	14	14	15	15	15	20
V_{pore} (cm^3/g)	1.21	0.36	0.21	0.15	0.91	0.46	0.35
			(D) MCF-HAS				
SA_{BET} (m^2/g)	229	147	136	60	135	100	95
d_{cell} (nm)	48	53	58	57	52	60	60
d_{window} (nm)	12	20	24	23	23	25	25
V_{pore} (cm^3/g)	1.49	1.13	0.84	0.35	1.19	0.94	0.88

initial capacity to the MCF-DMA adsorbent before steam treatment, but the MCF-PEI adsorbent showed a higher final CO_2 capacity after the steam treatments compared to the other two classes of adsorbents used in this study. The higher stability of the MCF-HAS and MCF-PEI sorbents after steam treatment suggests the potential for improved stability of PEI-containing materials in real steam stripping applications.

Finally, it should be noted that the CO_2 capacities of the all the adsorbents before and after treatment are relatively low compared to values reported in the literature (7, 54). This is associated with several factors, including (i) temperature, as the adsorption is carried out here at 45 °C instead of the typical 25 °C or room temperature; (ii) humidity, as the capacities were measured under dry conditions, with humidity always increasing CO_2 capacities with supported amine adsorbents; and (iii) equilibration time, as complete saturation may not be achieved for all adsorbents after 3 h of adsorption in TGA mode.

The decrease of the capacity of the adsorbents after various steam treatments may be associated with two primary causes. One is the collapse or destruction of the mesoporous structure of the substrate during steam treatment, and the other is chemical changes of the amine functional group associated with oxidation or other reactions during the steam treatment conditions. A third cause, loss of amine groups because of leaching of amines (53) via hydrolysis of substrate-organic bonds is not expected to play a large role in this case, as the steam treatment process is a batch process and there is thus minimal means to remove the organic species from the substrate. There is no washing, filtration, or other solid recovery process involved that would lead to significant loss of detached amines from the solid materials. Nonetheless, some minor amount of organic species may be lost by this mode, and such losses may account for the small weight changes described in Figure 1 after treatment at low temperatures in steam/nitrogen. Alternately, the observed minor loss of organic content under those conditions may in fact not be a loss of organic weight, and may instead reflect a decrease of other volatile species that might be lost in the 160−760 °C range during TGA experiments (e.g., water).

To address the potential for loss of CO_2 adsorption capacity due to microstructural changes of the substrate, we assessed all the adsorbents after the various steam treatments by nitrogen physisorption, and the results are summarized in Table 3. Cell and window pore size distributions were calculated using the Broekhoff-de Boer method with the Frenkel−Halsey−Hill (BdB-FHH) modification (80). As shown in Table 3, the BET surface areas and pore volumes of the as-synthesized amine-functionalized adsorbents were all lower compared to those of their counterpart bare MCF materials (Table 1), confirming the occupation of the mesopores in MCF by organic amine groups. Furthermore, after treatment of the adsorbents under various steaming conditions, it is evident in all cases that some microstructural destruction occurred, as denoted by the significant loss in BET surface area and pore volume, even under the mildest conditions. As expected, the loss in porosity became more significant as the steaming temperature was increased. For example, the as-prepared MCF-Mono adsorbent had a BET surface area of 289 m^2/g, an average pore volume of 1.85 cm^3/g, and average window and cell diameters of 12 and 49 nm. After treatment of the sample at 106 °C under steam/air conditions, the average window and cell diameter

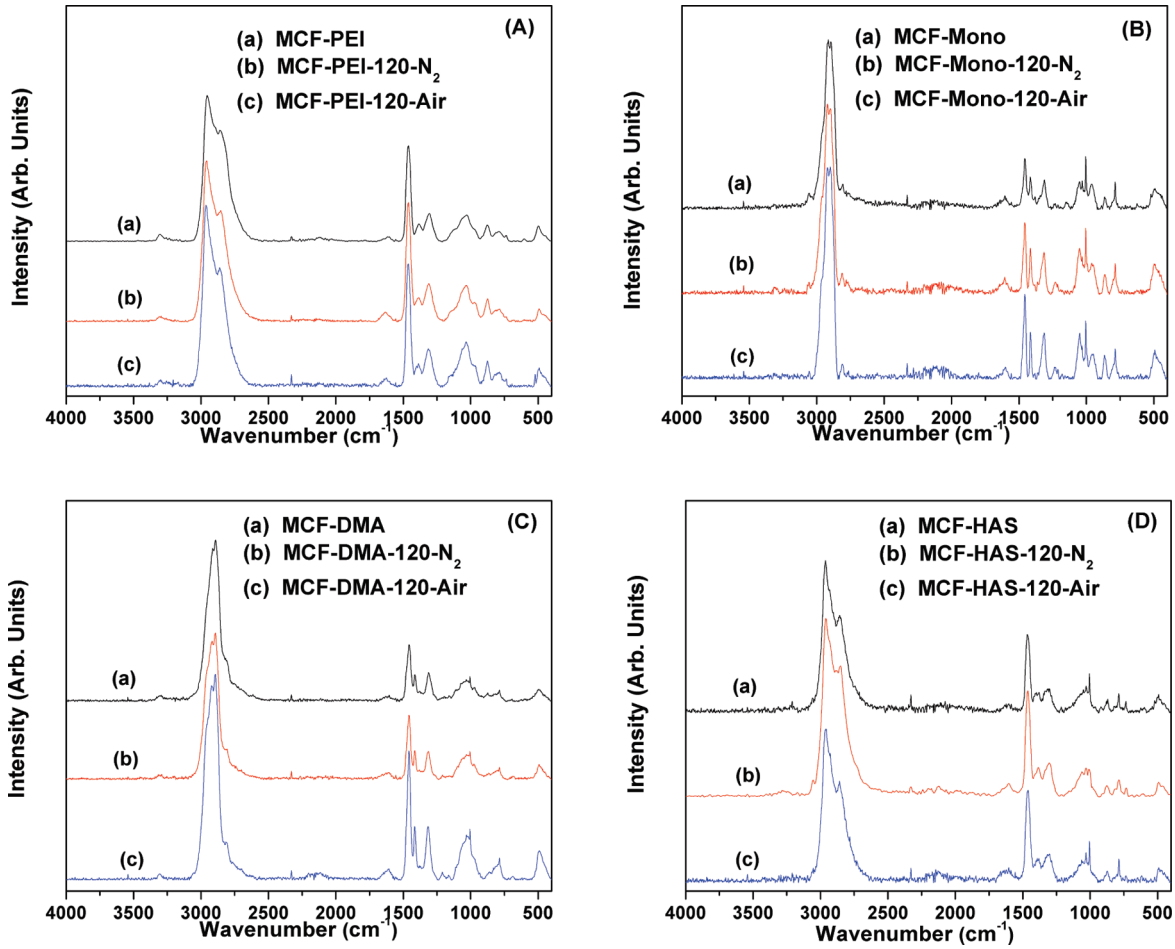

FIGURE 3. Comparison of FT-Raman spectra of various supported amine-based adsorbent before and after treatment in steam/air and steam/nitrogen at 120 °C.

increased to 24 and 52 nm, resulting in lower BET surface area (84 m^2/g) and smaller average pore volume (0.62 cm^3/g). The physisorption results on the bare MCF (Table 1) and various amine-functionalized MCF materials (Table 3) all support the hypothesis that treatment under steaming conditions resulted in significant degradation of the porosity of the substrate, leading to lower surface areas and pore volumes. This might be expected to result in a loss of accessible amine groups in the adsorbents, resulting in decreased CO_2 capacities after steaming. For the destruction of the MCF substrate, a similar trend of microstructure change was observed under both steam/air and steam/nitrogen conditions, indicating the oxygen present in air does not change the steam stability of the MCF substrate itself during steam treatment to a large extent, as expected. Furthermore, it is noteworthy that the porosity of the MCF-HAS sample was least affected by the treatments, again suggesting that the structure of this material, having aminopolymer covalently bound to the solid substrate, may serve to stabilize and protect the support during the treatments.

FTIR and FT-Raman spectroscopy measurements were carried out on the adsorbent materials before and after steam treatment to assess chemical changes in the surface functional groups. While the Raman spectra of the as synthesized and steam treated samples showed no distinct differences (Figure 3), the FTIR spectra for all samples treated in steam/air except for the MCF-Mono clearly showed the appearance of a new carbonyl stretch at 1710 cm^{-1} (Figure 4). This may be due to reaction with CO_2 or O_2 from ambient air. Drage et al. reported the formation of urea linkages when PEI impregnated adsorbents were exposed to pure CO_2 at temperatures greater than 135 °C under dry conditions (15). More recently, Sayari and co-workers reported the formation of urea linkages when monoamine and triamine grafted (class 2) as well as PEI impregnated (class 1) pore expanded MCM-41 materials were exposed to pure CO_2 under dry conditions (81). Urea formation was, however, not detected when the runs were carried out in the presence of water vapor. Recently, Bacsik et al. (82) also reported the carbonyl stretch at 1701 cm^{-1} in FTIR spectra as evidence of formation of carbamic acid groups associated with the reaction between amines and CO_2. However, in the case of the materials here, signals from adsorbed CO_2 would be expected to be strongest using the primary amine-containing sample MCF-Mono, as primary amines have the highest heat of adsorption with CO_2 and thus should extract the most CO_2 from the air, whereas in this work there was no peak at 1710 cm^{-1} associated with the MCF-Mono sample. Thus, it is not expected that this peak is primarily associated with CO_2 adsorption. Based on these 3 reports, we might expect to see carbonyl groups appearing only after treatment under dry conditions. Because in this study the

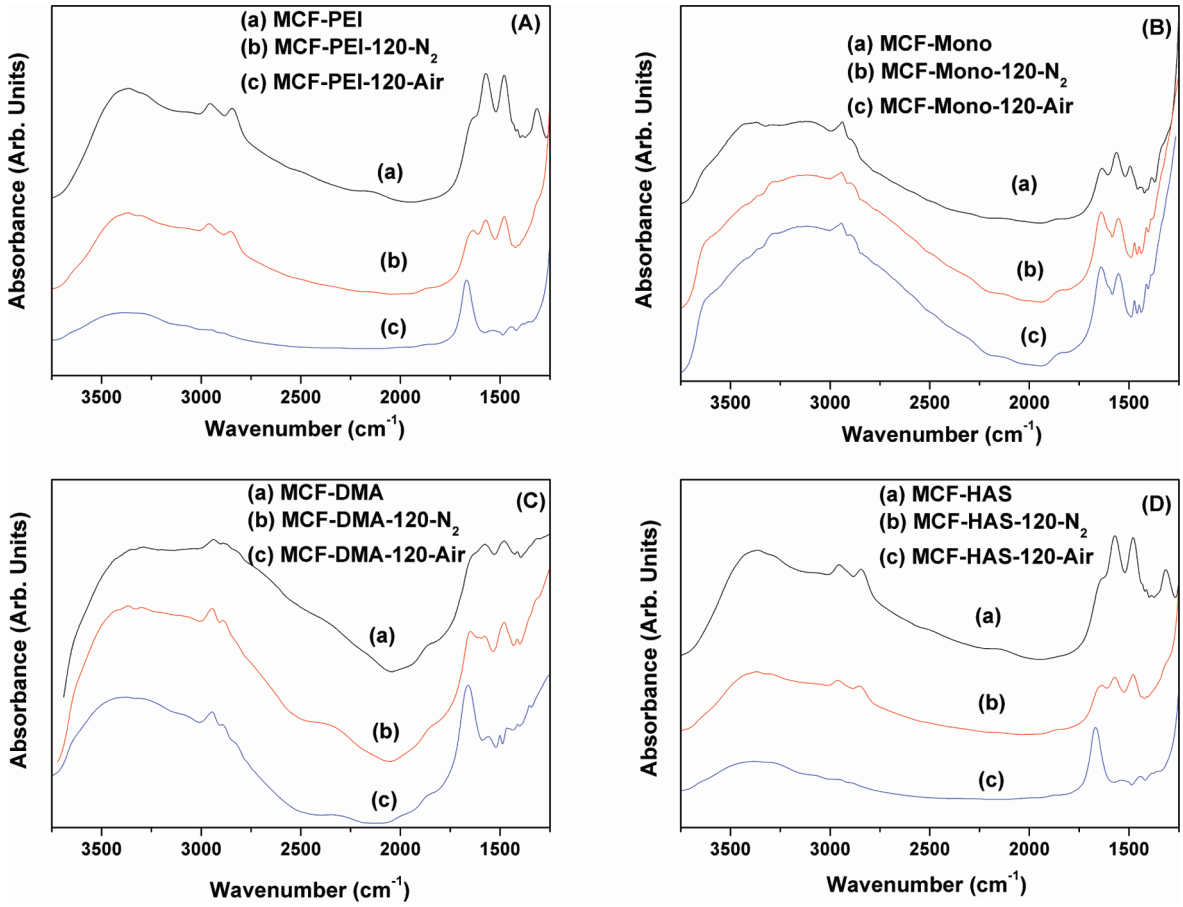

FIGURE 4. Comparison of FT-IR of various supported amine-based adsorbent before and after treatment in steam/air and steam/nitrogen at 120 °C.

carbonyl stretch can be observed for samples treated in the presence of steam and in the presence of parts per million level concentrations of CO_2 (distinct from the dry conditions used and exposure to concentrated CO_2 in the case of Drage and Sayari's reports 15, 81), it is more likely that this structural change of the surface functional groups on exposure to steam/air was a result of oxidative degradation. Furthermore, in support of this, the samples treated under steam/N_2 do not show any significant change in IR/Raman spectroscopic signatures. Nonetheless, the formation of carbonyl groups after treatment in air due to extraction of CO_2 from the ambient air cannot be formally ruled out, as there is excess CO_2 in the air contained inside the autoclave relative to the total amine content.

Also noteworthy is the C−H stretching region in the FT-Raman spectra (Figure 3). In all the spectra, the C−H stretching peaks in the 2800−3000 cm^{-1} range from all the adsorbents showed essentially no change after the steam treatments, indicating that the CH_2 groups were stable in both steam/air and steam/nitrogen conditions up to 120 °C. This result is consistent with the nearly constant organic content of all four adsorbents before and after steam treatment, as estimated by TGA measurements (Figure 2), because the carbon and hydrogen are main elements in the amine-based adsorbents, and no significant changes in organic content were observed after steam treatments in either air or nitrogen atmospheres in that temperature range (Figure 2). This might suggest that the slight hypothetical organic loss in the 100−120 °C range may not be a loss of organic content and instead a decrease in the amount of another volatile species such as water after the various treatments (vide supra).

CONCLUSIONS

Four amine-functionalized MCF adsorbents belonging to the three classes of solid amine CO_2 adsorbents were prepared and treated in both steam/air and steam/nitrogen conditions in an autoclave apparatus at various temperatures (106−180 °C) for 24 h. The apparent organic content and CO_2 capacity of the adsorbents decreased after steam treatment under both air and nitrogen atmospheres at the highest treatment temperatures. All samples showed a loss in CO_2 adsorption capacity after treatments at all temperatures, with the loss being higher at higher temperatures and with exposure to air. However, the bare support showed a significant loss in porosity and surface area after treatment in steam under all conditions as well. Thus, the loss in CO_2 capacity was associated with two independent factors (i) structural collapse of the thin-walled mesocellular foam silica supports and (ii) amine degradation due to exposure to steam and/or oxygen, and the two factors cannot be rigorously assessed independently based on the results of this first of its kind study. The extent and ubiquity of the structural collapse of the supports may suggest that this

factor played the major role in the loss of capacity after the treatments, although further studies are needed to confirm this conjecture. Indeed, a previous report of steam-stripping regeneration of supported amine adsorbents suggested that such materials were stable under steaming for short periods at 105 °C. However, most of the materials in that previous report were based on a different substrate, with the one example of an MCF support being akin to the most stable material reported here, MCF-HAS. This result is consistent with structural collapse playing the primary role in the capacity loss observed here after steam treatments. Clearly, however, oxygen from air can have some adverse effect, as in all cases the steam/nitrogen treatment had less impact on the CO_2 capacity than the steam/air treatment.

It is noteworthy that the MCF-PEI and MCF-HAS adsorbents showed better capacity stability compared to MCF-Mono and MCF-DMA adsorbents in both steam treatment conditions, with the MCF-DMA being the most affected. The overall steam stability ranking of the four adsorbents is: MCF-HAS > MCF-PEI > MCF-Mono > MCF-DMA under both steam/nitrogen and steam/air conditions. The results reported here provide a preliminary investigation of the steam stability of various supported amine adsorbents, and additional investigations are needed to decouple the impact of support stability and amine degradation, as well as to further assess the potential for practical application of steam stripping as a regeneration method of solid amine CO_2 adsorbents. Undoubtedly, oxide supports that are robust to steaming conditions are required for routine steam-stripping regeneration of supported amine adsorbents.

Acknowledgment. The authors acknowledge financial support from Global Thermostat, LLC. C.W.J. thanks support from the School of Chemical & Biomolecular Engineering at Georgia Tech via the J. Carl & Sheila Pirkle Faculty Fellowship. S.C. and C.W.J. thank the Dreyfus Foundation for support; S.C. is a Camille & Henry Dreyfus Foundation Post-Doctoral Fellow in Environmental Chemistry. P.B. and C.W.J. thank the King Abdullah University of Science and Technology (KAUST) for financial support the financial support through award KUS-I1-011-21. S.A.D. thanks DOE-NETL for financial support under Contract FE0002438.

REFERENCES AND NOTES

(1) Intergovernmental Panel on Climate Change. Summary for Policymakers. In *Climate Change 2007: The Physical Science Basis*; Cambridge University Press: Cambridge, U.K., 2007.
(2) Keith, D. W. *Science* **2009**, *325*, 1654–1655.
(3) Rochelle, G. T. *Science* **2009**, *325*, 1652–1654.
(4) Fluor Daniel. *Engineering and Economic Evaluation of CO_2 Removal from Fossil-Fuel-Fired Power Plants*; Report IE-7365; Electric Power Research Institute: Palo Alto, CA, 1991.
(5) St. Clair, J. H.; Simister, W. F. *Oil Gas J.* **1983**, *81*, 109–113.
(6) Arnold, D. S.; Barnett, D. A.; Isom, R. H. *Oil Gas J.* **1982**, *80*, 130–133.
(7) Choi, S.; Drese, J. H.; Jones, C. W. *ChemSusChem* **2009**, *2*, 796–854.
(8) Xu, X. C.; Song, C. S.; Andresen, J. M.; Miller, B. G.; Scaroni, A. W. *Energy Fuels* **2002**, *16*, 1463–1469.
(9) Wang, X. X.; Schwartz, V.; Clark, J. C.; Ma, X. L.; Overbury, S. H.; Xu, X. C.; Song, C. S. *J. Phys. Chem. C* **2009**, *113*, 7260–7268.
(10) Xu, X. C.; Song, C. S.; Andresen, J. M.; Miller, B. G.; Scaroni, A. W. *Microporous Mesoporous Mater.* **2003**, *62*, 29–45.
(11) Xu, X. C.; Song, C. S.; Miller, B. G.; Scaroni, A. W. *Ind. Eng. Chem. Res.* **2005**, *44*, 8113–8119.
(12) Xu, X. C.; Song, C. S.; Miller, B. G.; Scaroni, A. W. *Fuel Process. Technol.* **2005**, *86*, 1457–1472.
(13) Ma, X. L.; Wang, X. X.; Song, C. S. *J. Am. Chem. Soc.* **2009**, *131*, 5777–5783.
(14) Son, W. J.; Choi, J. S.; Ahn, W. S. *Microporous Mesoporous Mater.* **2008**, *113*, 31–40.
(15) Drage, T. C.; Arenillas, A.; Smith, K. M.; Snape, C. E. *Microporous Mesoporous Mater.* **2008**, *116*, 504–512.
(16) Yue, M. B.; Chun, Y.; Cao, Y.; Dong, X.; Zhu, J. H. *Adv. Funct. Mater.* **2006**, *16*, 1717–1722.
(17) Yue, M. B.; Sun, L. B.; Cao, Y.; Wang, Y.; Wang, Z. J.; Zhu, J. H. *Chem.—Eur. J.* **2008**, *14*, 3442–3451.
(18) Yue, M. B.; Sun, L. B.; Cao, Y.; Wang, Z. J.; Wang, Y.; Yu, Q.; Zhu, J. H. *Microporous Mesoporous Mater.* **2008**, *114*, 74–81.
(19) Franchi, R. S.; Harlick, P. J. E.; Sayari, A. *Ind. Eng. Chem. Res.* **2005**, *44*, 8007–8013.
(20) Tsuda, T.; Fujiwara, T. *J. Chem. Soc., Chem. Commun.* **1992**, 1659–1661.
(21) Tsuda, T.; Fujiwara, T.; Taketani, Y.; Saegusa, T. *Chem. Lett.* **1992**, 2161–2164.
(22) Angeletti, E.; Canepa, C.; Martinetti, G.; Venturello, P. *J. Chem. Soc., Perkin Trans.* **1989**, 105–107.
(23) Kundu, S. K.; Roy, S. K. *J. Lipid Res.* **1979**, *20*, 825–833.
(24) Airoldi, C.; Gushikem, Y.; Espinola, J. G. P. *Colloids Surf.* **1986**, *17*, 317–323.
(25) Khatri, R. A.; Chuang, S. S. C.; Soong, Y.; Gray, M. *Ind. Eng. Chem. Res.* **2005**, *44*, 3702–3708.
(26) Khatri, R. A.; Chuang, S. S. C.; Soong, Y.; Gray, M. *Energy Fuels* **2006**, *20*, 1514–1520.
(27) Brinker, C. J. Scherer, G. W. *Sol—Gel Science: The Physics and Chemistry of Sol—Gel Processing*; Academic Press: San Diego, 1990.
(28) Gray, M. L.; Soong, Y.; Champagne, K. J.; Pennline, H.; Baltrus, J. *Int. J. Environ. Technol. Manage.* **2004**, *4*, 82–88.
(29) Gray, M. L.; Soong, Y.; Champagne, K. J.; Pennline, H.; Baltrus, J. P.; Stevens, R. W.; Khatri, R.; Chuang, S. S. C.; Filburn, T. *Fuel Process. Technol.* **2005**, *86*, 1449–1455.
(30) Hiyoshi, N.; Yogo, K.; Yashima, T. *Microporous Mesoporous Mater.* **2005**, *84*, 357–365.
(31) Serna-Guerrero, R.; Da'na, E.; Sayari, A. *Ind. Eng. Chem. Res.* **2008**, *47*, 9406–9412.
(32) Knowles, G. P.; Delaney, S. W.; Chaffee, A. L. *Ind. Eng. Chem. Res.* **2006**, *45*, 2626–2633.
(33) Knowles, G. P.; Graham, J. V.; Delaney, S. W.; Chaffee, A. L. *Fuel Process. Technol.* **2005**, *86*, 1435–1448.
(34) Huang, H. Y.; Yang, R. T.; Chinn, D.; Munson, C. L. *Ind. Eng. Chem. Res.* **2003**, *42*, 2427–2433.
(35) Chang, A. C. C.; Chuang, S. S. C.; Gray, M.; Soong, Y. *Energy Fuels* **2003**, *17*, 468–473.
(36) Hiyoshi, N.; Yogo, K.; Yashima, T. *Chem. Lett.* **2004**, *33*, 510–511.
(37) Zelenak, V.; Halamova, D.; Gaberova, L.; Bloch, E.; Llewellyn, P. *Microporous Mesoporous Mater.* **2008**, *116*, 358–364.
(38) Kim, S.; Ida, J.; Guliants, V. V.; Lin, J. Y. S. *J. Phys. Chem. B* **2005**, *109*, 6287–6293.
(39) Knofel, C.; Descarpentries, J.; Benzaouia, A.; Zelenak, V.; Mornet, S.; Llewellyn, P. L.; Hornebecq, V. *Microporous Mesoporous Mater.* **2007**, *99*, 79–85.
(40) Wei, J.; Shi, J.; Pan, H.; Zhao, W.; Ye, Q.; Shi, Y. *Microporous Mesoporous Mater.* **2008**, *116*, 394–399.
(41) Zheng, F.; Tran, D. N.; Busche, B. J.; Fryxell, G. E.; Addleman, R. S.; Zemanian, T. S.; Aardahl, C. L. *Ind. Eng. Chem. Res.* **2005**, *44*, 3099–3105.
(42) Diaf, A.; Garcia, J. L.; Beckman, E. J. *J. Appl. Polym. Sci.* **1994**, *53*, 857–875.
(43) Diaf, A.; Beckman, E. J. *React. Funct. Polym.* **1995**, *27*, 45–51.
(44) Ochiai, B.; Yokota, K.; Fujii, A.; Nagai, D.; Endo, T. *Macromolecules* **2008**, *41*, 1229–1236.
(45) Franchi, R. S.; Harlick, P. J. E.; Sayari, A. *Ind. Eng. Chem. Res.* **2005**, *44*, 8007–8013.
(46) Harlick, P. J. E.; Sayari, A. *Ind. Eng. Chem. Res.* **2007**, *46*, 446–458.
(47) Harlick, P. J. E.; Sayari, A. *Ind. Eng. Chem. Res.* **2006**, *45*, 3248–3255.

(48) Harlick, P. J. E.; Sayari, A. *Stud. Surf. Sci. Catal.* **2005**, *158*, 987–994.
(49) Serna-Guerrero, R.; Da'na, E.; Sayari, A. *Ind. Eng. Chem. Res.* **2008**, *47*, 4761–4766.
(50) Belmabkhout, Y.; De Weireld, G.; Sayari, A. *Langmuir* **2009**, *25*, 13275–13278.
(51) Belmabkhout, Y.; Sayari, A. *Adsorption* **2009**, *15*, 318–328.
(52) Belmabkhout, Y.; Serna-Guerrero, R.; Sayari, A. *Ind. Eng. Chem. Res.* **2010**, *49*, 359–365.
(53) Hicks, J. C.; Drese, J. H.; Fauth, D. J.; Gray, M. L.; Qi, G. G.; Jones, C. W. *J. Am. Chem. Soc.* **2008**, *130*, 2902–2903.
(54) Drese, J. H.; Choi, S.; Lively, R. P.; Koros, W. J.; Fauth, D. J.; Gray, M. L.; Jones, C. W. *Adv. Funct. Mater.* **2009**, *19*, 3821–3832.
(55) Kim, J. H.; Moon, J. H.; Park, J. W. *J. Colloid Interface Sci.* **2000**, *227*, 247–249.
(56) Rosenholm, J.; Duchanoy, A.; Linden, M. *Chem. Mater.* **2008**, *20*, 1126–113.
(57) Rosenholm, J. M.; Pennikangas, A.; Linden, M. *Chem. Commun.* **2006**, *37*, 3901–3911.
(58) Li, W.; Choi, S.; Drese, J. H.; Hornbostel, M.; Krishnan, G.; Eisenberger, P. M.; Jones, J. W. *ChemSusChem* **2010**, *3*, 899–903.
(59) Xia, Y.; Mokaya, R. *J. Phys. Chem. B* **2003**, *107*, 6954–6960.
(60) Chen, L. Y.; Jaenicke, S.; Ghuah, G. K. *Microporous Mater.* **1997**, *12*, 323–330.
(61) Zhang, F. Q.; Yan, Y.; Yang, H. F.; Meng, Y.; Yu, C. Z.; Tu, B.; Zhao, D. Y. *J. Phys. Chem. B* **2005**, *109*, 8723–8732.
(62) Galarneau, A.; Driole, M. F.; Petitto, C.; Chiche, B.; Bonelli, B.; Armandi, M.; Onida, B.; Garrone, E.; Renzo, F. D.; Fajula, F. *Microporous Mesoporous Mater.* **2005**, *83*, 172–180.
(63) Yang, H. Q.; Zhang, G. Y.; Hong, X. L.; Zhu, Y. Y. *Microporous Mesoporous Mater.* **2004**, *68*, 119–125.
(64) Yamamoto, K.; Tatsumi, T. *Chem. Lett.* **2000**, *6*, 624–625.
(65) Park, D. H.; Nishiyama, N.; Egashira, Y.; Ueyama, K. *Ind. Eng. Chem. Res.* **2001**, *40*, 6105–6110.
(66) Ping, E. W.; Wallace, R.; Pierson, J.; Fuller, T. F.; Jones, C. W. *Microporous Mesoporous Mater.* **2010**, *132*, 174–180.
(67) Lettow, J. S.; Han, Y. J.; Schmidt-Winkel, P.; Yang, P. D.; Zhao, D. Y.; Stucky, G. D.; Ying, J. Y. *Langmuir* **2000**, *16*, 8291–8295.
(68) Wystrach, V. P.; Kaiser, D. W.; Schaefer, F. C. *J. Am. Chem. Soc.* **1955**, *77*, 5915–5918.
(69) Li, Q.; Wu, Z.; Feng, D.; Tu, B.; Zhao, D. *J. Phys. Chem. C.* **2010**, *114*, 5012–5019.
(70) Schmidt-Winkel, P.; Lukens, W. W.; Yang, P.; Margolese, D. I.; Lettow, J. S.; Ying, J. Y.; Stucky, G. D. *Chem. Mater.* **2000**, *12*, 686–696.
(71) Schmidt-Winkel, P.; Lukens, W. W.; Zhao, D.; Yang, P.; Chmelka, B. F.; Stucky, G. D. *J. Am. Chem. Soc.* **1999**, *121*, 254–255.
(72) Beck, J. S.; VartUli, J. C.; Roth, W. J.; Leonowicz, M. E.; Kresge, C. T.; Schmitt, K. D.; Chu, C. T.; Olson, D. H.; Sheppard, E. W.; McCullen, S. B.; Higgins, J. B.; Schlenker, J. L. *J. Am. Chem. Soc.* **1992**, *114*, 10834–10843.
(73) Zhao, D.; Feng, J.; Huo, Q.; Melosh, N.; Fredickson, G. H.; Chmelka, B. F.; Stucky, G. D. *Science* **1998**, *279*, 548–552.
(74) Corma, A. *Chem. Rev.* **1997**, *97*, 2373–2419.
(75) Herbert, R.; Wang, D.; Schomacker, R.; Schlogl, R.; Hess, C. *ChemPhysChem* **2009**, *10*, 2230–2233.
(76) Garcia, A.; Colilla, M.; Izquierdo-Barba, I.; Vallet-Regi, M. *Chem. Mater.* **2009**, *21*, 4135–4145.
(77) Zhang, F.; Yan, Y.; Yang, H.; Meng, Y.; Yu, C.; Tu, B.; Zhao, D. *J. Phys. Chem. B.* **2005**, *109*, 8723–8732.
(78) Carniato, F.; Bisio, C.; Paul, G.; Gatti, G.; Bertinetti, L.; Coluccia, S.; Marchese, L. *Mater. Chem.* **2010**, *26*, 5504–5509.
(79) Li, D. F.; Su, D. S.; Song, J. W.; Guan, X. Y.; Hofmann, K.; Xiao, F. S. *J. Mater. Chem.* **2005**, *15*, 5063–5069.
(80) Lukens, W. W.; Schmidit-Winkel, P.; Zhao, D.; Feng, J.; Stucky, G. D. *Langmuir* **1999**, *15*, 5403–5409.
(81) Sayari, A.; Belabkhout, Y. *J. Am. Chem. Soc.* **2010**, *132*, 6312–6314.
(82) Bacsik, Z.; Atlur, R.; Garcia-Bennett, A. E.; Hedin, N. *Lnagmuir* **2010**, *12*, 10013–10024.

AM100786Z